Clinical Radiology 76 (2021) 627.e13–627.e21

Contents lists available at ScienceDirect

Clinical Radiology

journal homepage: www.clinicalradiologyonline.net

Radiomics-based model for predicting pathological complete response to neoadjuvant chemotherapy in muscle-invasive bladder cancer

S.J. Choi [a], K.J. Park [a,*], C. Heo [b], B.W. Park [b], M. Kim [a], J.K. Kim [a]

[a] Department of Radiology, Asan Medical Center, University of Ulsan College of Medicine, Seoul, Republic of Korea
[b] Institute for Life Sciences, University of Ulsan College of Medicine, Seoul, 05505, Republic of Korea

ARTICLE INFORMATION

Article history:
Received 4 September 2020
Received in revised form
21 December 2020
Accepted 11 February 2021

AIM: To develop and validate a radiomics-based model for predicting response to neoadjuvant chemotherapy (NAC) using baseline computed tomography (CT) images in patients with muscle-invasive bladder cancer (MIBC).

MATERIALS AND METHODS: A radiomics signature for predicting pathological complete response (pCR) was developed using radiomics features selected by a random forest classifier on baseline CT images, and imaging predictors were identified in the training set (87 patients). By incorporating imaging predictors and radiomics signature, an imaging-based model was constructed using multivariate logistic regression analysis and validated in an independent validation set consisting of 48 patients with CT from outside institutions. The performance and clinical usefulness of the imaging-based model for predicting pCR were evaluated using area under the receiver operating characteristic curve (AUC) and decision curve analysis. Using a cut-off determined in the training set, the positive likelihood ratios of the imaging-based model were calculated and compared with imaging and histological predictors.

RESULTS: The radiomics signature was developed based on six stable radiomics features. An imaging-based model incorporating radiomics signature, tumour shape, tumour size, and clinical stage showed good performance for predicting pCR in both the training (AUC, 0.85; 95% confidence interval [CI], 0.78–0.93) and validation (AUC, 0.75; 95% CI, 0.60–0.86) sets, providing a larger net benefit in decision curve analysis. The imaging-based model showed a higher positive likelihood ratio (1.91) for pCR than imaging and histological predictors (1.33–1.63).

CONCLUSIONS: The radiomics-based model using baseline CT images may predict the response of patients with MIBC to NAC.

* Guarantor and correspondent: K. J. Park, Department of Radiology, Asan Medical Center, University of Ulsan College of Medicine, 88, Olympic-ro 43-gil, Songpa-gu, Seoul 05505, Republic of Korea. Tel.: +82 2 3010 0132; fax: +82 2 476 4719.
E-mail address: kyejin629@gmail.com (K.J. Park).

https://doi.org/10.1016/j.crad.2021.03.001
0009-9260/

Introduction

Neoadjuvant chemotherapy (NAC) followed by radical cystectomy (RC) is currently the standard of care for patients with muscle-invasive bladder cancers (MIBCs), as these have significantly improved overall survival and pathological downstaging.[1,2] The pathological response to NAC is an important marker for predicting survival outcomes,[3,4] as patients with pathological complete response (pCR) have shown better overall survival outcomes than patients with pathological residual disease; however, staged-matched analysis has shown that patients with pathological residual disease have poorer survival outcomes when treated with NAC and RC rather than with RC alone,[5] making the prediction of response to NAC and the stratification of patients clinically important in optimising outcomes of patients with MIBC.

The close relationship between pathological tumour response to NAC and survival outcomes in patients with MIBC highlights the need to develop and utilise reliable predictors. Responses to NAC vary and may be associated with the underlying biological behaviour of the tumour, as well as initial stage at diagnosis.[6,7] The ability of several genetic and molecular tests, including tests of genetic alterations, DNA repair mechanisms, and molecular subtyping of basal and luminal tumours, to predict pathological response to NAC in patients with MIBC has been intensively investigated.[8–12] In addition, some histological variants have been associated with sensitivity to chemotherapy, with sarcomatoid carcinomas being chemo-resistant, and small cell and lymphoepithelioma-like carcinomas being chemo-sensitive.[13] To date, however, the ability of imaging biomarkers, which are non-invasive and of relatively low cost, to predict response to NAC using baseline computed tomography (CT) has not been investigated.[7] To the authors' knowledge, only few studies have evaluated the ability of dynamic contrast-enhanced magnetic resonance imaging (MRI)[14] or radiomics and a deep-learning approach[15,16] to predict response to treatment in patients with MIBC, and they were based on pre- and post-chemotherapy images. Response prediction using baseline CT may have important clinical implications in deciding the treatment strategy.

Radiomics is a process by which a large number of quantitative parameters are extracted from imaging data, enabling the quantitative analysis of tumours and providing diagnostic, prognostic, and predictive information.[17–19] Radiomic features can represent tumour properties such as spatial heterogeneity and potential linkage to genomic alterations and tumoural or peritumoural microenvironments, which are closely related to the response to treatment.[20–22] Radiomics quantification of tumour heterogeneity in conjunction with clinical and imaging predictors may be useful to predict treatment response to NAC in patients with MIBC, providing a decision-support tool for determining treatment plans. In this regard, the present study was performed to develop and validate a radiomics-based imaging model incorporating a radiomics signature and other imaging characteristics for predicting the response of MIBC patients to NAC.

Materials and methods

Study population

The study was approved by the institutional review board at Asan Medical Center, which waived the requirement for informed consent because of the retrospective design of the study.

A review of the electronic database of Asan Medical Center identified 477 patients who underwent radical or partial cystectomy for MIBC between January 2013 and February 2020. Patients were included if they underwent NAC, followed by RC or partial cystectomy and pelvic lymphadenectomy; if baseline computed tomography (CT) images were available before chemotherapy; and if CT showed tumours >1 cm in diameter. Of the 235 eligible patients, those who underwent baseline CT before NAC at Asan Medical Center were assigned to the training set (Fig 1). For external validation, patients who underwent CT at baseline, consisting of variable and heterogeneous CT techniques at outside institutions between January 2013 and January 2018 were assigned to the independent validation set. Consequently, 135 patients were included, including 87 (mean age, 69.4 years; range, 49–89 years) in the training set and 48 (mean age, 67.9 years; range, 34–86 years) in the validation set.

Pathological assessment of response

Pathological treatment response after transurethral resection of bladder tumour (TURB) and subsequent NAC were evaluated on the cystectomy specimens, with the official pathology report used as the reference standard. In Asan Medical Center, the cystectomy specimens were evaluated by two pathologists, including an expert pathologist specialising in genitourinary pathology. Pathologically proven absence of tumour (ypT0) was considered as a pCR.

Image acquisition, segmentation, and feature extraction

CT images of patients in the training set were obtained during the portal venous phase, 80 seconds after intravenous administration of a contrast agent. The detailed CT protocol of Asan Medical Center is provided in Electronic Supplementary Material, Data S1. CT techniques used for patients in the validation set varied, and detailed information was lacking, because the CT images were obtained from 48 different institutions.

Bladder tumours were segmented independently by two radiologists, including one fellowship-trained genitourinary radiologist (K.J.P. and S.J.C. with 8 and 4 years of experience, respectively, in interpretation of oncological images). Both radiologists were blinded to clinical information and treatment outcomes. Regions of interest (ROIs) were drawn

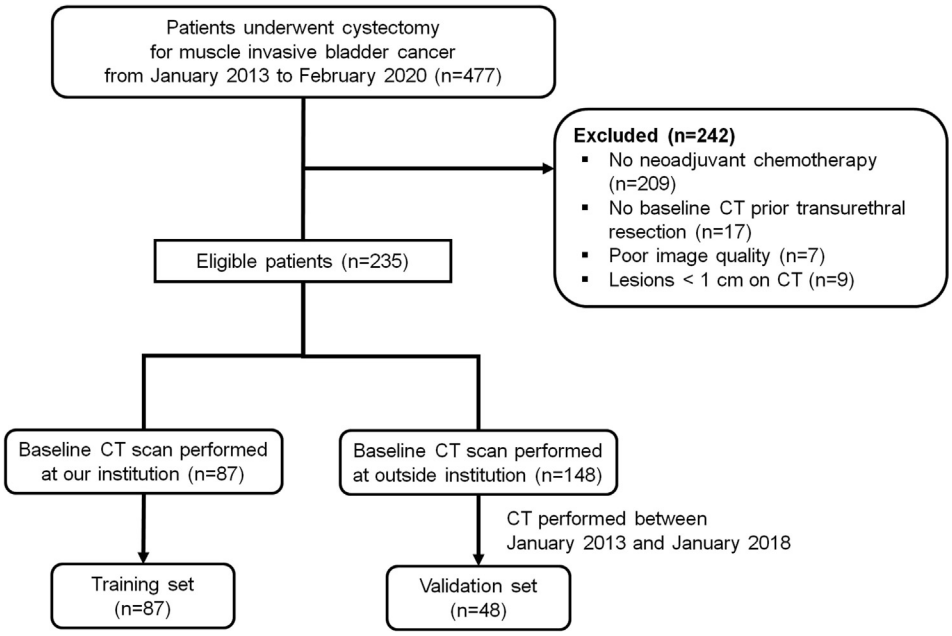

Figure 1 Flow diagram of patient inclusion.

manually using open-source software (MITK; available at www.mitk.org).

A total of 419 RFs were extracted from all manually segmented lesions[23,24] using an in-house software package (AsanFEx). These 419 RFs included 14 morphological features, six local intensity features, 54 intensity-based statistical features, 60 intensity histogram features, 75 grey-level co-occurrence, and 48 grey-level run length matrix features, 48 grey-level size zone matrix, 48 grey-level distance zone matrix, 15 neighbourhood grey-tone difference matrix, and 51 neighbouring grey-level dependence based features.

Selection of reproducible features for construction of a radiomics signature

To build the radiomics signature, robust RFs were chosen by a three step process to ensure reproducibility.[21,25,26] The first step was to assess the reproducibility of the image segmentation process by each of the two readers. Features showing a concordance correlation coefficient (CCC) $\geq$0.70 were considered reliable. Of the 419 RFs, 86 (20.5%) were considered reliable on the image segmentation process.

In the second step, highly correlated features, defined as having Pearson correlation coefficients $>$0.75, were removed, leading to the selection of 14 representative features with the smallest mean absolute correlations. In the third step, each feature was ranked by its importance using a random forest classifier.[27] Finally, a radiomics signature predictive of pCR was constructed from the top selected features by multivariate logistic regression.

Evaluation of baseline imaging and clinical characteristics

Semantic features, which were evaluated by a radiologist specialising in genitourinary images (K.J.P.) based on baseline CT images of bladder tumours, included tumour diameter, enhancement pattern (homogeneous or heterogeneous), and shape (infiltrative or mass-forming). Clinical stage (T2, T3b, or T4) was also evaluated based on baseline CT findings. In addition, demographic characteristics (age and sex), TURB state (incomplete or complete), trigone or bladder neck involvement of the tumour, presence of hydronephrosis, multiplicity of lesions, and suspicious lymph nodes on CT were also evaluated, that have been reported to represent poorer outcomes.[28] Also evaluated was the presence of variant histology (i.e., plasmacytoid, squamous, glandular, or micropapillary components), which has been reported to be associated with clinical outcome and response to chemotherapy.[12,13] Significant clinical, histological, and imaging parameters, including age, sex, TURB state (incomplete or complete), presence of variant histology, semantic features, clinical stage, and radiomics signature in the training set, were identified by univariate and multivariable logistic regression analyses. Thereafter, significant semantic features and radiomics signature were used to develop imaging-based model using a multivariate logistic regression to predict pCR.

Statistical analysis

Differences in demographic characteristics in the training and validation sets were compared using Student's *t*-tests for continuous variables and the chi-square test or Fisher's exact test for categorical variables. The reproducibility of radiomics features on image segmentation was assessed by measuring CCC, with a CCC $>$0.70 considered reproducible. The predictive performance of the radiomics signature and imaging-based model was evaluated by receiver operating characteristic (ROC) curve analysis of the training and validation sets. The optimal cut-off for differentiating low from high probability of pCR was determined using the Youden *J*

index on the training set. The diagnostic performance of the imaging-based model was assessed in the independent validation set by calculating the sensitivity, specificity, correct classification rate, and positive and negative likelihood ratios of the cut-off value determined in the training set. Positive and negative likelihood ratios were calculated as sensitivity/(1-specificity) and (1-sensitivity)/specificity, respectively. Decision curve analysis was used to calculate the net benefit from the radiomics signature and imaging-based model at different threshold probabilities in the validation set.[29] The threshold for statistical significance was set at $p<0.05$. All statistical analyses were performed using R statistical software (version 3.6.2; R foundation for Statistical Computing, Vienna, Austria).

Results

Patient outcomes

The baseline clinical characteristics of patients in the training and validation sets are summarised in Table 1 pCR after TURB and NAC was achieved by 34 (39.1%) of 87 patients in the training set and 20 (41.7%) of 48 patients in the validation set. The clinical characteristics of these two sets of patients were similar, except that the frequency of hydronephrosis was significantly higher in the training set ($p=0.001$).

Table 1
Baseline demographics and clinical characteristics of the patients.

	Training set ($n=87$)	Validation set ($n=48$)	p-Value
Age (y)†	69.4 ± 9.5	67.9 ± 12.3	0.42
Sex			0.69
Male	73 (83.9%)	39 (81.2%)	
Female	14 (16.1%)	9 (19.8%)	
Tumour diameter (mm)[a]	36.7 ± 16.2	36.7 ± 14.0	0.99
Clinical stage			0.19
T2	37 (42.5%)	26 (54.2%)	
T3b and T4	50 (57.5%)	22 (45.8%)	
Trigone/bladder neck involvement	51 (58.6%)	23 (47.9%)	0.23
Presence of hydronephrosis	36 (41.4%)	6 (12.5%)	0.001
Multiplicity			0.70
Single	57 (65.5%)	33 (68.8%)	
Multiple	30 (34.5%)	15 (31.2%)	
Transurethral resection of tumour			0.35
Incomplete	56 (64.4%)	27 (56.3%)	
Complete	31 (35.6%)	21 (43.8%)	
Type of surgery			0.83
Radical cystectomy	75 (86.2%)	42 (87.5%)	
Partial cystectomy	12 (13.8%)	6 (12.5%)	
Presence of variant histology			0.43
Pure urothelial carcinoma	64 (73.6%)	39 (81.3%)	
Variant histology	23 (26.4%)	9 (18.8%)	
Pathological response			0.77
Complete response	34 (39.1%)	20 (41.7%)	
Pathological residual disease	53 (60.9%)	28 (58.3%)	
Event			
Progression	26 (29.9%)	17 (35.45%)	0.51
Death	24 (27.6%)	16 (33.3%)	0.48

[a] Data are presented as mean ± standard deviation.

Development of radiomics signature for predicting pathological complete response

Fig. 2 shows the workflow used to develop a radiomics signature and imaging-based model in the present study. The three steps of the feature selection process identified the six most reliable features to predict pCR; these included one first-order feature (local intensity peak) and five second-order features (dependence count non-uniformity normalised, dependence count non-uniformity, low grey-level count emphasis, busyness, and large distance emphasis; Table 2, Electronic Supplementary Material, Fig. S1). These six RFs were used in multivariable logistic regression analysis to construct a radiomics signature.

Clinical and imaging predictors of pCR

Table 3 shows the results of univariate and multivariate logistic regression analyses to identify clinical and imaging variables predictive of pCR. Univariate analysis showed that higher normalised radiomics signature (hazard ratio [HR], 3.856; $p<0.001$) and complete TURB (HR, 3.46; $p=0.008$) were associated with a significantly higher probability of pCR. By comparison, older age (HR, 0.95; $p=0.037$), male sex (HR, 0.29; $p=0.042$), large baseline tumour size (HR, 0.94; $p=0.001$), infiltrative tumour shape (HR, 0.35; $p=0.023$), higher clinical stage (T3b or T4 *versus* T2; HR, 0.41; $p=0.046$), presence of variant histology (HR, 0.160; $p=0.006$), trigone or bladder neck involvement (HR, 0.30; $p=0.009$), and positive lymph nodes on CT (HR, 0.21; $p=0.003$) were associated with a significantly lower probability of pCR. Multivariate analysis revealed that older age (HR, 0.85; $p=0.003$), infiltrative shape (HR, 0.16; $p=0.028$), presence of variant histology (HR, 0.05; $p=0.012$), trigone or bladder neck involvement (HR, 0.09; $p=0.005$), and positive lymph nodes on CT (HR, 0.098; $p=0.023$) were independently associated with pathological residual disease after TURB and NAC, whereas a higher radiomics signature was a significant independent predictor of pCR (HR, 6.05; $p=0.001$). Representative examples of pCR and pathological residual disease are presented in Electronic Supplementary Material Figs. S2 and S3.

Predictive performance and clinical use of radiomics signature and imaging-based model

Univariate analysis of imaging features to predict pCR led to the construction of an imaging-based model using radiomics signature, tumour shape, clinical stage (T2, T3b, or T4), and tumour size using the following equation:

$$\frac{p}{1-p} = \exp(-0.90 + 5.25 \bullet radiomicssignature - 0.14 \bullet infiltrativeshapeatbaseline - 0.33 \bullet T3bstage + 0.66 \bullet T4stage - 0.036 \bullet tumordiameter)$$

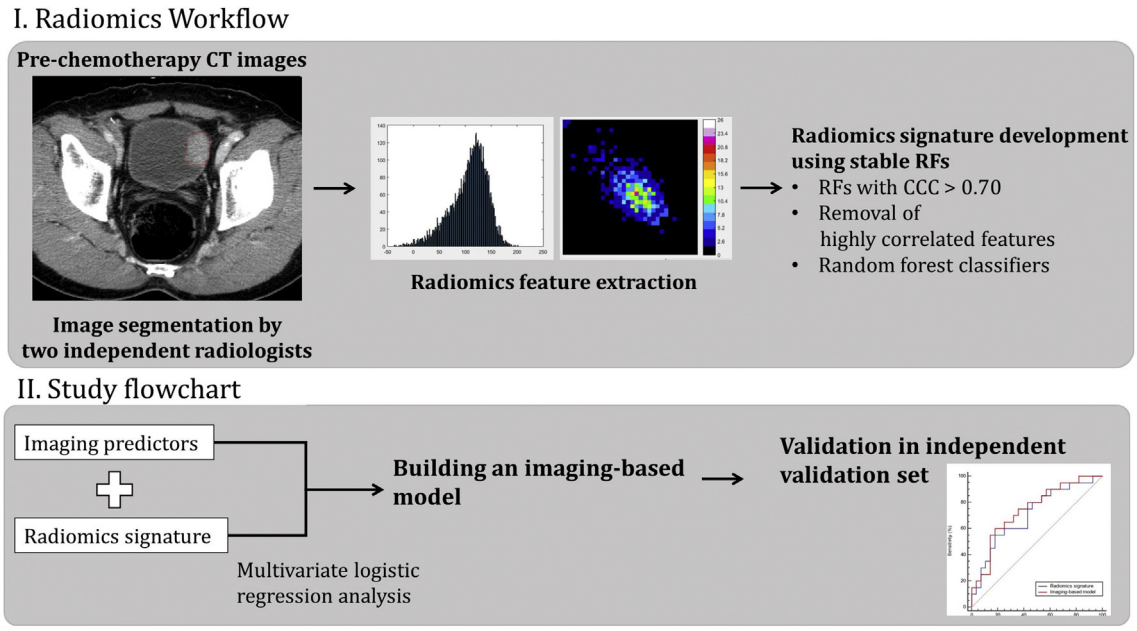

Figure 2 Workflow in the current study.

where *p*=the probability of pCR predicted by the imaging-based model.

The AUCs of the radiomics signature in predicting pCR were 0.79 (95% confidence interval [CI], 0.70–0.89) in the training set and 0.71 (95% CI, 0.55–0.86) in the independent validation set, which consisted of heterogeneous CT scans obtained at different institutions using different imaging protocols. In addition, the AUCs of the imaging-based model for predicting pCR were 0.85 (95% CI, 0.78–0.93) in the training set and 0.75 (95% CI, 0.60–0.86) in the validation set (Fig 3a).

Decision curve analysis showed that the radiomics signature and the imaging-based model had higher net benefits than without use of predictive model (i.e., a treat-all or treat-none strategy) in predicting pCR across the reasonable threshold probabilities (Fig 3b).

Table 2
Radiomics signature based on the top six features selected by a random forest classifier to predict pathological complete response after neoadjuvant chemotherapy in patients with muscle-invasive bladder cancer.

Feature name	Feature type	Mean reduction in impurity (%)
Dependence count non-uniformity normalised	NGLDF	2.02
Dependence count non-uniformity	NGLDF	1.82
Low grey-level count emphasis	NGLDF	1.52
Busyness	NGTDF	1.45
Local intensity peak	Local intensity feature	1.43
Large distance emphasis	GLDZF	1.38

NGLDF, neighboring grey-level dependence-based feature; NGTDF, neighborhood grey tone difference-based feature; GLDZF, grey-level distance zone-based feature.

The optimal cut-off determined in the training set was 0.3023 based on the Youden *J* index. Using this cut-off, the response prediction using the imaging-based model had the highest positive likelihood ratio in the validation set (1.91; 95% CI, 1.13–3.23), compared with tumour shape (1.40; 95% CI, 0.95–2.06), clinically organ-confined disease (cT2, 1.63; 95% CI, 0.98–2.73), and variant histology (1.33; 95% CI, 1.03–1.72; Table 4).

Discussion

In patients with MIBC, a pCR to NAC is associated with better survival outcomes and is therefore significant prognostically.[3] Because a delay in surgery in non-responders has a potentially negative impact on patient survival, the identification of predictive markers to stratify patients who would benefit from NAC would be important clinically.[11] The present study identified clinical and imaging characteristics associated with outcomes following NAC for MIBC. This led to the development and validation of an imaging-based model using baseline CT images to predict response in patients treated with NAC for MIBC. The construction of this imaging-based model was based on semantic and radiomics features, including clinical stage, tumour size, tumour shape, and radiomics signature. This model showed a greater ability to predict pCR, with higher positive and lower negative likelihood ratios, than evaluation by clinical staging, tumour shape, or the presence of variant histology. Moreover, this model demonstrated a clinical net benefit than without model use. This imaging-based model could identify patients who would benefit from NAC, thus providing decision support.

Randomised clinical trials have shown that NAC has clinical benefits in patients with MIBC, including improved overall survival and pathological downstaging of the

Table 3
Univariate and multivariate logistic regression analyses of clinical and imaging factors predictive of pathological complete response to neoadjuvant chemotherapy.

	Univariate			Multivariate		
	HR	95% CI	*p*-Value	HR	95% CI	P
Age	0.950	0.905, 0.997	0.037[a]	0.847	0.760, 0.944	0.003†
Male sex	0.289	0.088, 0.956	0.042[a]	0.157	0.017, 1.442	0.102
Tumour characteristics at CT						
Baseline tumour diameter	0.939	0.905, 0.975	0.001[a]	0.990	0.914, 1.072	0.807
Heterogeneous enhancement	0.866	0.349, 2.150	0.756			
Infiltrative shape	0.345	0.138, 0.861	0.023[a]	0.163	0.032, 0.820	0.028†
Clinical stage			0.046[a]			
T2	Reference			Reference		
T3b or T4	0.406	0.168, 0.983		1.958	0.347, 11.037	0.446
Complete TURB	3.462	1.381, 8.680	0.008[a]	1.090	0.230, 5.171	0.913
Presence of variant histology	0.160	0.043, 0.591	0.006[a]	0.046	0.004, 0.506	0.012†
Trigone/bladder neck involvement	0.303	0.123, 0.745	0.009[a]	0.087	0.016, 0.486	0.005†
Hydronephrosis	0.433	0.174, 1.079	0.072			
Multiplicity	0.434	0.166, 1.135	0.089			
LN positive	0.206	0.073, 0.580	0.003[a]	0.098	0.013, 0.730	0.023†
Radiomics signature [b]	3.856	2.063, 7.205	<0.001[a]	6.045	2.039, 17.921	0.001†

[a] Statistically significant.
[b] Z-score normalisation was performed in the training set.

tumour.[1,2] The current standard treatment for MIBC consists therefore of NAC followed by RC. Response to NAC may be an important indicator of survival outcome, as a meta-analysis showed that pCR was associated with better survival outcomes than pathological residual disease.[3] Although NAC is thought to reduce the tumour burden of micrometastatic disease, there have been concerns about unnecessary delays of definitive surgery in non-responders to NAC and the possible overtreatment of patients who do not have micrometastatic disease.[30] Because responses to NAC differ in patients with different histological, genetic, and molecular characteristics, reliable markers predicting response to NAC are essential to optimise individual patient outcomes.[9–12,31,32] Despite several attempts to predict and understand the divergent biological responses to NAC in patients with MIBC, including analyses of gene expression and histology,[8,12] few studies have attempted to identify imaging-based predictors that can be obtained easily and non-invasively; one study used radiomics and another used deep-learning algorithms based on pre- and post-treatment CT to predict treatment response.[15,33] Response prediction should ideally be based on baseline images, considering the clinical implications of whether to choose neoadjuvant chemotherapy followed by RC or upfront surgery. In this regard, acceptable performance in the prediction of response following NAC using only baseline CT is noteworthy, especially when other studies used both baseline and post-treatment images to predict the response.[15,33]

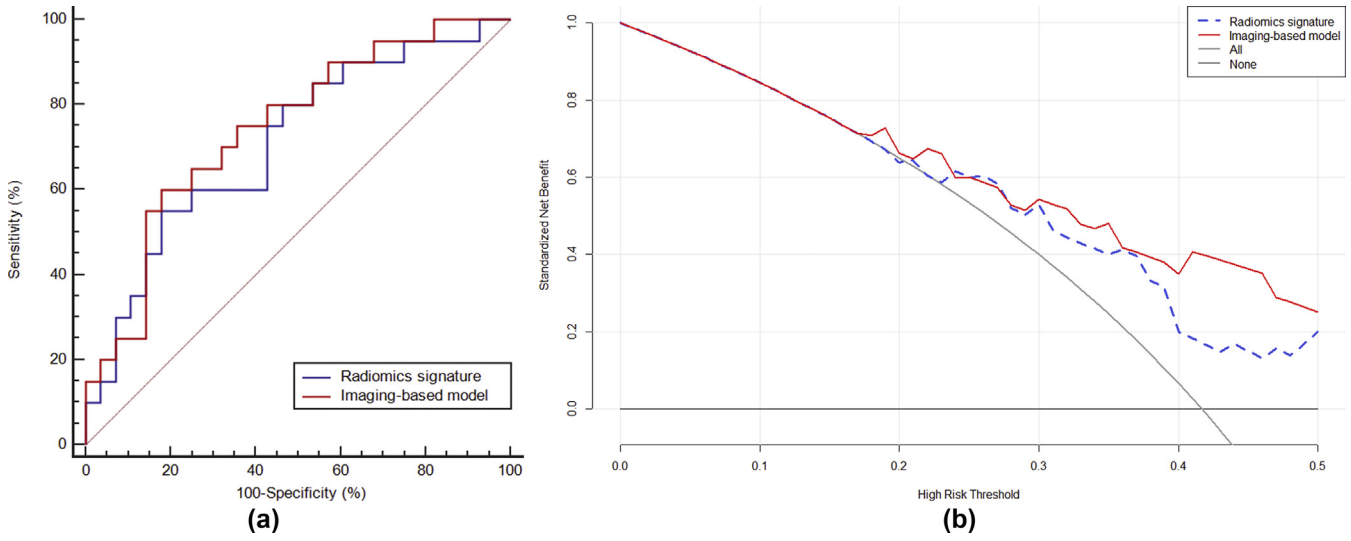

Figure 3 ROC curve and decision curve analysis of the radiomics signature and the imaging-based model in the validation set. (a) The AUCs for predicting pathological complete response were 0.71 (95% CI, 0.55–0.86) for the radiomics signature and 0.75 (95% CI, 0.60–0.86) for the imaging-based model in the validation set. (b) The *y*-axis represents the net benefit. The decision curve demonstrates that the imaging-based model and radiomics signature showed a higher net benefit compared with no prediction model use, across the range of threshold probabilities.

Table 4
Performances of imaging and histological features and of an imaging-based model in the validation set for prediction of pathological complete response.

Modality	Sensitivity (%)	Specificity (%)	Correct classification rate (%)	Positive LR[a]	Negative LR[a]	AUC†
Mass-forming shape	80.0 (16/20)	42.9 (12/28)	58.3	1.40 (0.95–2.06)	0.47 (0.18–1.24)	0.61 (0.46, 0.75)
Clinical T2 stage	70.0 (14/20)	57.1 (16/28)	62.5	1.63 (0.98–2.73)	0.53 (0.25–1.10)	0.64 (0.48, 0.77)
Variant histology	95.0 (19/20)	28.6 (8/28)	56.3	1.33 (1.03–1.72)	0.18 (0.02–1.29)	0.62 (0.47, 0.75)
Imaging-based model	75.0 (15/20)	60.7 (17/28)	66.7	1.91 (1.13–3.23)	0.41 (0.18–0.93)	0.75 (0.60, 0.86)

Unless otherwise indicated, data in parentheses are numerator/denominator.
[a] Data in parentheses are 95% confidence intervals.

Prediction of pathological response to NAC and TURB in cystectomy specimen should be based on multifactorial approach, including tumour biological characteristics related to chemo-sensitivity (including variant histology), tumour size, tumour shape, TURB procedure, and tumour stage at baseline.[1,7,13,34] Because the complete TURB procedure can contribute to pCR in approximately 38% of patients who achieve pCR,[34] pCR can be attributed to the morphological characteristics that tend to allow complete TURB procedures, as well as to the chemo-sensitivity of these tumours. The present non-invasive imaging-based model incorporating imaging-based tumour characteristics, including radiomics signature, tumour size, tumour shape, and clinical stage at baseline, demonstrated acceptable predictive performance (AUC, 0.75) and clinical benefit in decision curve analysis in the independent validation set. This model showed better performance than the currently used clinical and histological parameters, and can provide a comprehensive tool to predict pCR following TURB and NAC in patients with MIBC.

Bladder cancers with heterogeneous and coarse radiomics features (e.g., higher value in dependence count non-uniformity, large distance emphasis, or busyness) and presence of necrosis (higher value in low grey-level count emphasis) were associated with pathological residual disease. By contrast, homogeneous and highly enhancing (higher local intensity peak) tumours with evenly distributed grey-levels were associated with pCR.[24,35] Although this spatial heterogeneity based on radiomics features was not validated biologically or molecularly in the present study, the translational linkage of radiomics features with genomics or phenotypes to better understand variations in biological behaviour and to predict patient outcomes has been explored in patients with bladder cancer.[15,19,20,36,37] The radiomics-based approach in bladder cancer showed promising associations with angiogenesis,[20] which plays a leading role in the survival and metastatic potential of malignant tumours.[38] Because it reflects angiogenesis and ischaemic necrosis on CT,[39] the radiomics signature used in this study may provide insights into understanding bladder tumour biology, including intra-tumour heterogeneity, angiogenesis, and ischaemic necrosis, which may be closely linked to responses to NAC.

Radiomics can help predict responses to chemotherapy, immunotherapy, or radiotherapy in various diseases[22,40,41]; however, several radiomics features are redundant and non-reproducible, being highly dependent on the image acquisition technique (i.e., peak kilovoltage, tube current, or administration of contrast medium), image segmentation, and feature extraction methods.[26,35,42] Because radiomics features can be affected by multiple parameters, the reproducibility and generalisability of radiomics studies from different scanners and institutions have been questioned.[43,44] Thus, selection of robust and stable features is a crucial step for generalised use.[35] Furthermore, because they are highly correlated, radiomics features are likely to be clustered, thus violating the assumption of independence and affecting diagnostic performance.[45] To overcome this problem, stable features on image segmentation process were selected and highly correlated features were eliminated. These steps resulted in acceptable performance of the model in predicting response to NAC in the independent validation set, consisting of heterogeneous images from several institutions differing in their image acquisition and reconstruction processes. This radiomics signature and imaging-based model can generally be used in other institutions.

Recently, immunotherapy for neoadjuvant therapy for MIBC has demonstrated promising results, even in patients with variant histology of MIBC (i.e., squamous cell and lymphoepithelioma-like carcinoma), and those with tumours with high mutational burden and high programmed death ligand-1 (PD-L1) expression, who have been considered poor responders to conventional chemotherapy.[46,47] In this regard, biomarkers such as the molecular subtype and alterations in DNA damage repair genes may guide the utilisation of chemotherapeutic agents.[48] Likewise, imaging-driven approach including radiomics or deep learning algorithms is expected to help patients choose conventional agents or immunotherapy, to achieve a better tumour response.[33] Further studies are required to address this issue for tailored treatment in patients with MIBC.

This study had several limitations. First, the training set involved patients at a single institution, and the number of included patients was relatively small. Small sample sizes in radiomics studies are related to concerns about high dimensionality and risk of overfitting.[45] To compensate for the small sample size, redundant features that were less reproducible in the image segmentation process were excluded and highly correlated features were reduced. Moreover, the results were validated in an independent set of patients, consisting of heterogeneous CT data from multiple outside institutions; however, prospective, multicentre studies involving large numbers of patients are

needed to generalise the results. Further multicentre studies consisting of various imaging protocols and variable demographics of patient cohorts are required to generalise the use of radiomics-derived biomarkers. Second, biological and genomic validations were not included in this study. Further studies incorporating genomics and radiomics are needed to verify the associations between spatial heterogeneity and genetic variations. Moreover, images were segmented manually in this study, which can be labour-intensive and challenging for radiomics and can also be less reproducible compared with semiautomatic or automatic methods.[49] Although robust radiomics features that were less susceptible to image segmentation were selected, further efforts are required for the use of semi-automatic or automatic segmentation.

In conclusion, the present study identified useful imaging predictors and developed a radiomics-based imaging prediction model using baseline CT data. This model may be a promising tool to improve decision making and to facilitate individualised treatment in patients with MIBC. This non-invasive imaging-based model demonstrated the potential to predict pCR in a validation set, consisting of CT images obtained by heterogeneous protocols at outside institutions. In conjunction with clinical parameters and currently used genomic analysis, this imaging-based model could be useful in determining treatment strategies for patients with MIBC.

Conflict of interest

The authors declare no conflict of interest.

Acknowledgements

This work was supported by the Basic Science Research Program through the National Research Foundation of Korea (NRF) funded by the Ministry of Education, Science and Technology (2017R1A2B3007567) and through the Korea Health Industry Development Institute (KHIDI) funded by the Ministry of Health & Welfare, Republic of Korea (HI14C1090).

Appendix A. Supplementary data

Supplementary data to this article can be found online at https://doi.org/10.1016/j.crad.2021.03.001.

References

1. Grossman HB, Natale RB, Tangen CM, *et al*. Neoadjuvant chemotherapy plus cystectomy compared with cystectomy alone for locally advanced bladder cancer. *N Engl J Med* 2003;**349**(9):859–66.
2. Rosenblatt R, Sherif A, Rintala E, *et al*. Pathological downstaging is a surrogate marker for efficacy and increased survival following neoadjuvant chemotherapy and radical cystectomy for muscle-invasive urothelial bladder cancer. *Eur Urol* 2012;**61**(6):1229–38.
3. Petrelli F, Coinu A, Cabiddu M, *et al*. Correlation of pathological complete response with survival after neoadjuvant chemotherapy in bladder cancer treated with cystectomy: a meta-analysis. *Eur Urol* 2014;**65**(2):350–7.
4. Zargar H, Zargar-Shoshtari K, Lotan Y, *et al*. Final pathological stage after neoadjuvant chemotherapy and radical cystectomy for bladder cancer-does pT0 predict better survival than pTa/Tis/T1? *J Urol* 2016;**195**(4 Pt 1):886–93.
5. Bhindi B, Frank I, Mason RJ, *et al*. Oncologic outcomes for patients with residual cancer at cystectomy following neoadjuvant chemotherapy: a pathological stage-matched analysis. *Eur Urol* 2017;**72**(5):660–4.
6. Gakis G. Management of muscle-invasive bladder cancer in the 2020s: challenges and perspectives. *Eur Urol Focus* 2020;**6**(4):632–8.
7. Harzstark A, Merchant M. Identifying predictors of pathological complete response to neoadjuvant chemotherapy for muscle invasive bladder cancer. *J Clin Oncol* 2019;**37**(Suppl). e16015-e16015.
8. Seiler R, Gibb EA, Wang NQ, *et al*. Divergent biological response to neoadjuvant chemotherapy in muscle-invasive bladder cancer. *Clin Cancer Res* 2019;**25**(16):5082–93.
9. Groenendijk FH, de Jong J, Fransen van de Putte EE, *et al*. ERBB2 mutations characterize a subgroup of muscle-invasive bladder cancers with excellent response to neoadjuvant chemotherapy. *Eur Urol* 2016;**69**(3):384–8.
10. Lotan Y, Boorjian SA, Zhang J, *et al*. Molecular subtyping of clinically localized urothelial carcinoma reveals lower rates of pathological upstaging at radical cystectomy among luminal tumours. *Eur Urol* 2019;**76**(2):200–6.
11. Plimack ER, Dunbrack RL, Brennan TA, *et al*. Defects in DNA repair genes predict response to neoadjuvant cisplatin-based chemotherapy in muscle-invasive bladder cancer. *Eur Urol* 2015;**68**(6):959–67.
12. Voskuilen CS, Oo HZ, Genitsch V, *et al*. Multicenter validation of histopathological tumour regression grade after neoadjuvant chemotherapy in muscle-invasive bladder carcinoma. *Am J Surg Pathol* 2019;**43**(12):1600–10.
13. Lobo N, Shariat SF, Guo CC, *et al*. What is the significance of variant histology in urothelial carcinoma? *Eur Urol Focus* 2020;**6**(4):653–63.
14. Chakiba C, Cornelis F, Descat E, *et al*. Dynamic contrast enhanced MRI-derived parameters are potential biomarkers of therapeutic response in bladder carcinoma. *Eur J Radiol* 2015;**84**(6):1023–8.
15. Cha KH, Hadjiiski L, Chan HP, *et al*. Bladder cancer treatment response assessment in CT using radiomics with deep-learning. *Sci Rep* 2017;**7**(1):8738.
16. Meyer AB, Nichols P, Kates M, *et al*. SUO 2017: inaccuracy of clinical staging after neoadjuvant chemotherapy for muscle invasive bladder cancer. Available at: https://www.urotoday.com/conference-highlights/suo-2017/suo-2017-bladder-cancer/100286-suo-2017-inaccuracy-of-clinical-staging-after-neoadjuvant-chemotherapy-for-muscle-invasive-bladder-cancer.html [Accessed 26 June 2020].
17. Avanzo M, Stancanello J, El Naqa I. Beyond imaging: the promise of radiomics. *Phys Med* 2017;**38**:122–39.
18. Shaish H, Aukerman A, Vanguri R, *et al*. Radiomics of MRI for pretreatment prediction of pathological complete response, tumour regression grade, and neoadjuvant rectal score in patients with locally advanced rectal cancer undergoing neoadjuvant chemoradiation: an international multicenter study. *Eur Radiol* 2020 Nov;**30**(11):6263–73.
19. Wu S, Zheng J, Li Y, *et al*. A radiomics nomogram for the preoperative prediction of lymph node metastasis in bladder cancer. *Clin Cancer Res* 2017;**23**(22):6904–11.
20. Lin P, Wen D-y, Chen L, *et al*. A radiogenomics signature for predicting the clinical outcome of bladder urothelial carcinoma. *Eur Radiol* 2020;**30**(1):547–57.
21. Park JE, Kim HS, Park SY, *et al*. Prediction of core signaling pathway by using diffusion- and perfusion-based MRI radiomics and next-generation sequencing in isocitrate dehydrogenase wild-type glioblastoma. *Radiology* 2020;**294**(2):388–97.
22. Braman NM, Etesami M, Prasanna P, *et al*. Intratumoural and peritumoural radiomics for the pretreatment prediction of pathological complete response to neoadjuvant chemotherapy based on breast DCE-MRI. *Breast Cancer Res* 2017;**19**(1):57.
23. van Griethuysen JJM, Fedorov A, Parmar C, *et al*. Computational radiomics system to decode the radiographic phenotype. *Cancer Res* 2017;**77**(21):e104–7.
24. Zwanenburg ALS, Vallières M, Löck S, *et al*. Image biomarker standardisation initiative. Standardized quantitative radiomics for high-throughput image-based phenotyping. *Radiology* 2020 May;**295**(2):328–38.

25. Park KJ, Lee JL, Yoon SK, *et al*. Radiomics-based prediction model for outcomes of PD-1/PD-L1 immunotherapy in metastatic urothelial carcinoma. *Eur Radiol* 2020;**30**(10):5392–403.
26. Park BW, Kim JK, Heo C, *et al*. Reliability of CT radiomic features reflecting tumour heterogeneity according to image quality and image processing parameters. *Sci Rep* 2020;**10**(1):3852.
27. Breiman L. Random forests. *Machine Learn* 2001;**45**(1):5–32.
28. Spiess PE, Agarwal N, Bangs R, *et al*. Bladder cancer, version 5.2017, NCCN clinical practice guidelines in oncology. *J Natl Compr Cancer Netw* 2017;**15**(10):1240–67.
29. Steyerberg EW, Vickers AJ. Decision curve analysis: a discussion. *Med Decis Making* 2008;**28**(1):146–9.
30. Alfred Witjes J, Lebret T, Compérat EM, *et al*. Updated 2016 EAU guidelines on muscle-invasive and metastatic bladder cancer. *Eur Urol* 2017;**71**(3):462–75.
31. Van Allen EM, Mouw KW, Kim P, *et al*. Somatic ERCC2 mutations correlate with cisplatin sensitivity in muscle-invasive urothelial carcinoma. *Cancer Discov* 2014;**4**(10):1140–53.
32. Choi W, Porten S, Kim S, *et al*. Identification of distinct basal and luminal subtypes of muscle-invasive bladder cancer with different sensitivities to frontline chemotherapy. *Cancer Cell* 2014;**25**(2):152–65.
33. Wu E, Hadjiiski LM, Samala RK, *et al*. Deep learning approach for assessment of bladder cancer treatment response. *Tomography (Ann Arbor, Mich)* 2019;**5**(1):201–8.
34. Brant A, Kates M, Chappidi MR, *et al*. Pathological response in patients receiving neoadjuvant chemotherapy for muscle-invasive bladder cancer: is therapeutic effect owing to chemotherapy or TURBT? *Urol Oncol* 2017;**35**(1):34.e17–25.
35. Rizzo S, Botta F, Raimondi S, *et al*. Radiomics: the facts and the challenges of image analysis. *Eur Radiol Exp* 2018;**2**(1):36.
36. Ge L, Chen Y, Yan C, *et al*. Study progress of radiomics with machine learning for precision medicine in bladder cancer management. *Front Oncol* 2019;**9**. 1296-1296.
37. Zhang X, Xu X, Tian Q, *et al*. Radiomics assessment of bladder cancer grade using texture features from diffusion-weighted imaging. *J Magn Reson Imaging* 2017;**46**(5):1281–8.
38. Pinto A, Redondo A, Zamora P, *et al*. Angiogenesis as a therapeutic target in urothelial carcinoma. *Anticancer Drugs* 2010;**21**(10):890–6.
39. Jiang M, Lu HY, Shan XH, *et al*. CT quantitative analysis study for angiogenesis, and degree of ischaemic necrosis and glucose metabolite in non-small cell lung cancer. *Eur Rev Med Pharmacol Sci* 2018;**22**(13):4146–55.
40. Horvat N, Veeraraghavan H, Khan M, *et al*. MR imaging of rectal cancer: radiomics analysis to assess treatment response after neoadjuvant therapy. *Radiology* 2018;**287**(3):833–43.
41. Trebeschi S, Drago SG, Birkbak NJ, *et al*. Predicting response to cancer immunotherapy using noninvasive radiomic biomarkers. *Ann Oncol* 2019;**30**(6):998–1004.
42. Berenguer R, Pastor-Juan MDR, Canales-Vazquez J, *et al*. Radiomics of CT features may be nonreproducible and redundant: influence of CT acquisition parameters. *Radiology* 2018;**288**(2):407–15.
43. Mackin D, Fave X, Zhang L, *et al*. Measuring computed tomography scanner variability of radiomics features. *Invest Radiol* 2015;**50**(11):757–65.
44. Yasaka K, Akai H, Mackin D, *et al*. Precision of quantitative computed tomography texture analysis using image filtering: a phantom study for scanner variability. *Medicine (Baltimore)* 2017;**96**(21):e6993.
45. Park JE, Park SY, Kim HJ, *et al*. Reproducibility and generalizability in radiomics modeling: possible strategies in radiologic and statistical perspectives. *Korean J Radiol* 2019;**20**(7):1124–37.
46. Necchi A, Raggi D, Gallina A, *et al*. Updated results of PURE-01 with preliminary activity of neoadjuvant pembrolizumab in patients with muscle-invasive bladder carcinoma with variant histologies. *Eur Urol* 2020;**77**(4):439–46.
47. Necchi A, Anichini A, Raggi D, *et al*. Pembrolizumab as neoadjuvant therapy before radical cystectomy in patients with muscle-invasive urothelial bladder carcinoma (PURE-01): an open-label, single-arm, phase II study. *J Clin Oncol* 2018;**36**(34):3353–60.
48. Lenis AT, Lec PM, Chamie K, *et al*. Bladder cancer: a review. *JAMA* 2020;**324**(19):1980–91.
49. Parmar C, Rios Velazquez E, Leijenaar R, *et al*. Robust radiomics feature quantification using semiautomatic volumetric segmentation. *PLoS ONE* 2014;**9**(7):e102107.